

SUPPORTING INFORMATION

Structural and Kinetic Changes to Small-Pore Cu-Zeolites After Hydrothermal Aging Treatments and Selective Catalytic Reduction of NO_x with Ammonia

Jonatan D. Albarracin-Caballero^{1,†}, Ishant Khurana^{1,†}, John R. Di Iorio¹, Arthur J. Shih¹, Joel E. Schmidt², Michiel Dusselier^{2,3}, Mark E. Davis², Aleksey Yezerets⁴, Jeffrey T. Miller¹, Fabio H. Ribeiro^{1,*}, Rajamani Gounder^{1,*}

¹*Charles D. Davidson School of Chemical Engineering, Purdue University, 480 Stadium Mall Drive, West Lafayette, IN 47907, USA*

²*Chemical Engineering, California Institute of Technology, 1200 E. California Boulevard, MC 210-41, Pasadena, CA 91125, USA*

³*Center for Surface Chemistry and Catalysis, KU Leuven, Celestijnenlaan 200F, 3001 Heverlee, Belgium*

⁴*Cummins Inc., 1900 McKinley Ave., MC 50183, Columbus, IN 47201, USA*

*Corresponding authors. E-mail: rgounder@purdue.edu, fabio@purdue.edu

†J.D.A.-C. and I.K. contributed equally to this work.

Section S.1. Powder X-ray diffraction patterns on H- and Cu-zeolites

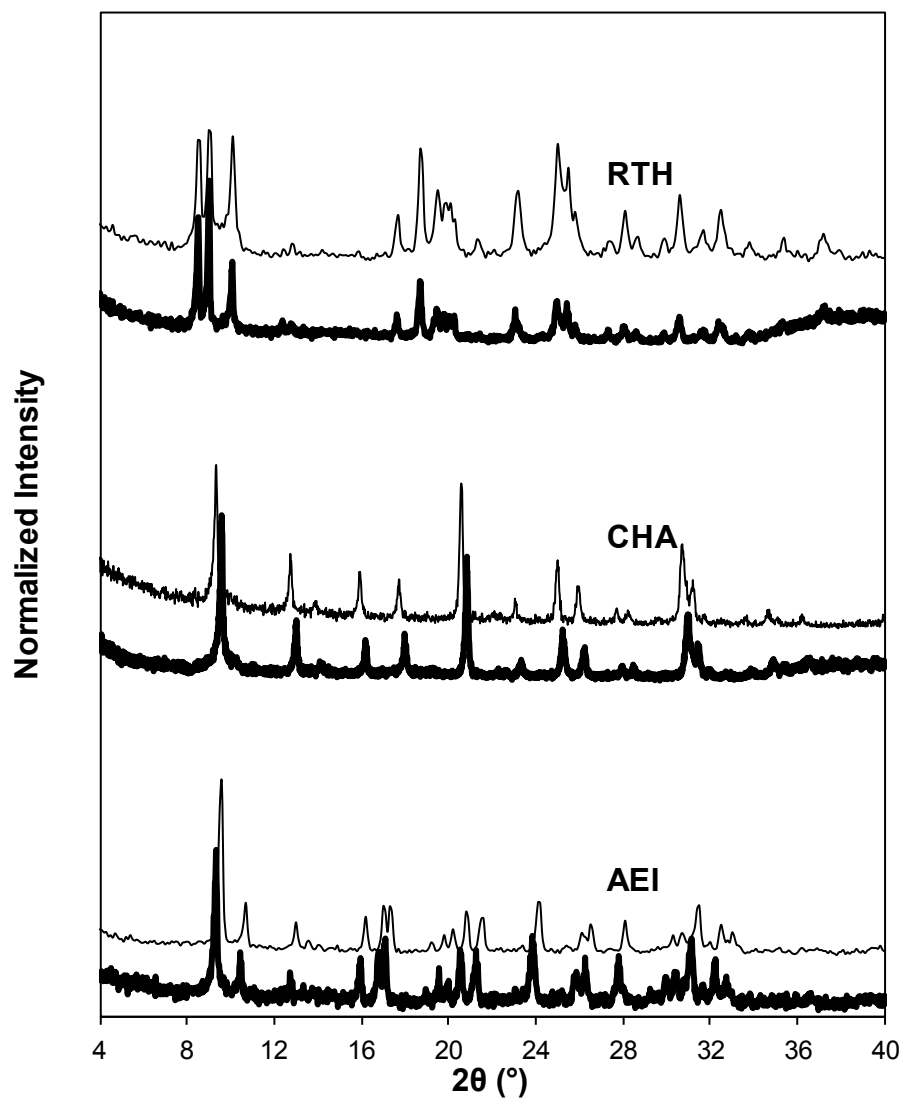


Figure S.1. XRD patterns of H-form (dark) and Cu-form (light) AEI, CHA, and RTH zeolites. Diffraction patterns are normalized so that the maximum peak intensity in each pattern is unity.

Section S.2. Argon adsorption isotherms on H- and Cu-zeolites

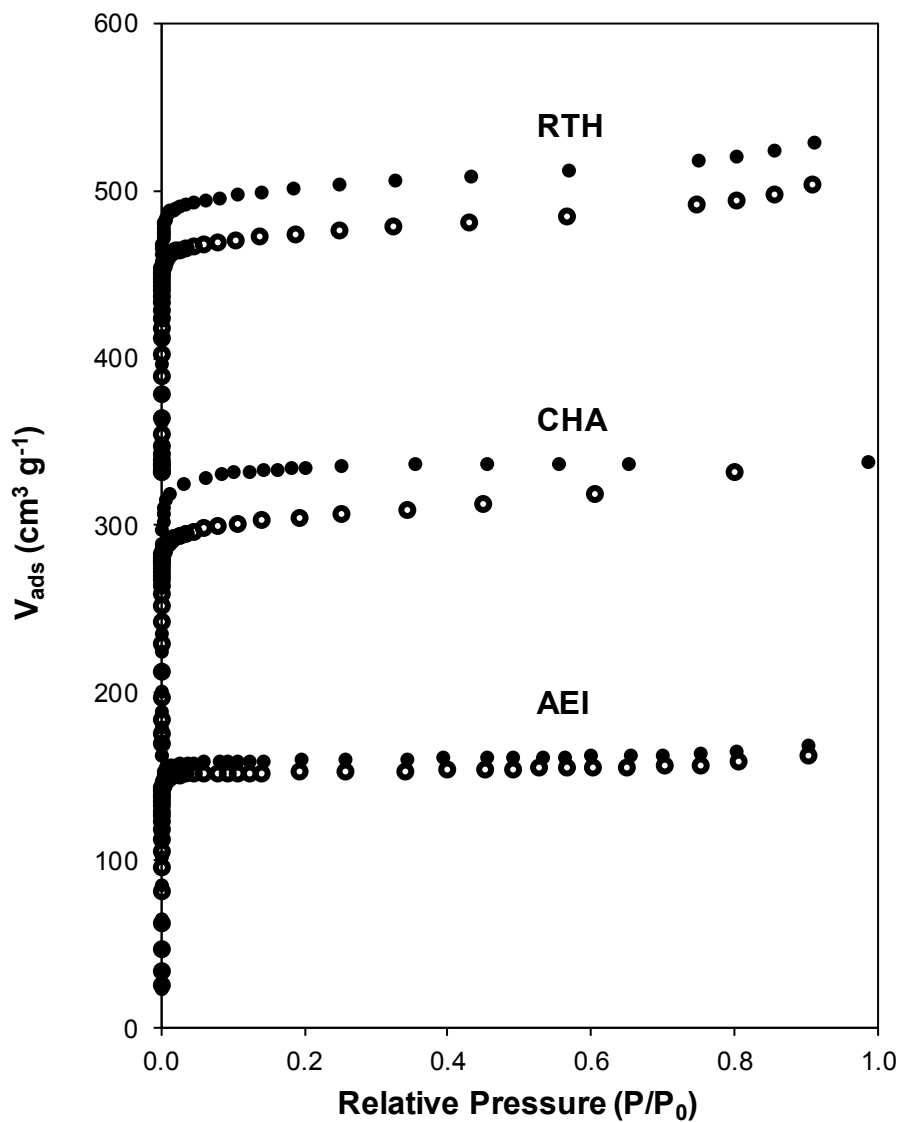


Figure S.2. Ar adsorption isotherms (87 K) on H-form (filled) and Cu-form (open) RTH, CHA and AEI zeolites. Adsorption isotherms are vertically offset (CHA: $160 \text{ cm}^3 \text{ g}^{-1}$, RTH: $320 \text{ cm}^3 \text{ g}^{-1}$) for clarity.

Section S.3. ^{27}Al MAS NMR spectra on H- and Cu-zeolites

^{27}Al MAS NMR spectra were measured on the H- and Cu-forms of the three zeolites in this study, AEI (Figure S.3.1), CHA (Figure S.3.2) and RTH (Figure S.3.3), in order to estimate the distribution of framework (Al_f) and extra-framework (Al_{ex}) Al species. NMR lines centered at 60 ppm were present for tetrahedral Al for RTH, and a small shoulder for penta-coordinated $\text{Al}^{1,2}$ was present for CHA and AEI. The tetrahedral along with distorted tetrahedral and penta-coordinated Al NMR lines were integrated together to estimate the total number of Al_f species, although we recognize difficulties in quantifying Al_f content from NMR spectra, because some species can reversibly change between tetrahedral and octahedral coordination depending on the conditions of the measurement³⁻⁵, and some extraframework alumina may also contain tetrahedrally-coordinated Al.^{1,6} The Al NMR lines centered at 0 ppm for octahedral Al were taken to reflect Al_{ex} species. Spectra of H- and Cu- form zeolites show Al incorporated predominantly into tetrahedral framework positions, with $\text{Al}_f/\text{Al}_{tot}$ values given in Table 2 of the main text.

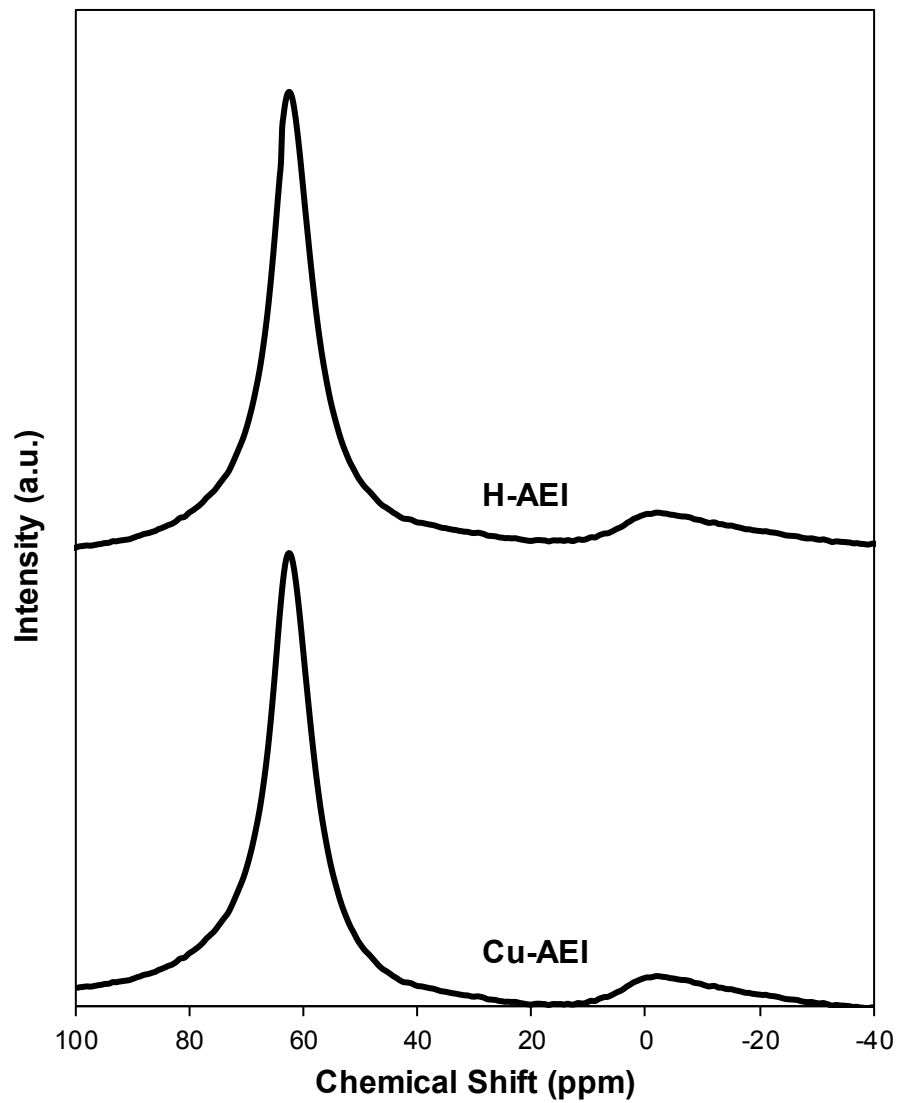


Figure S.3.1. ^{27}Al MAS NMR spectra of H-AEI and Cu-AEI.

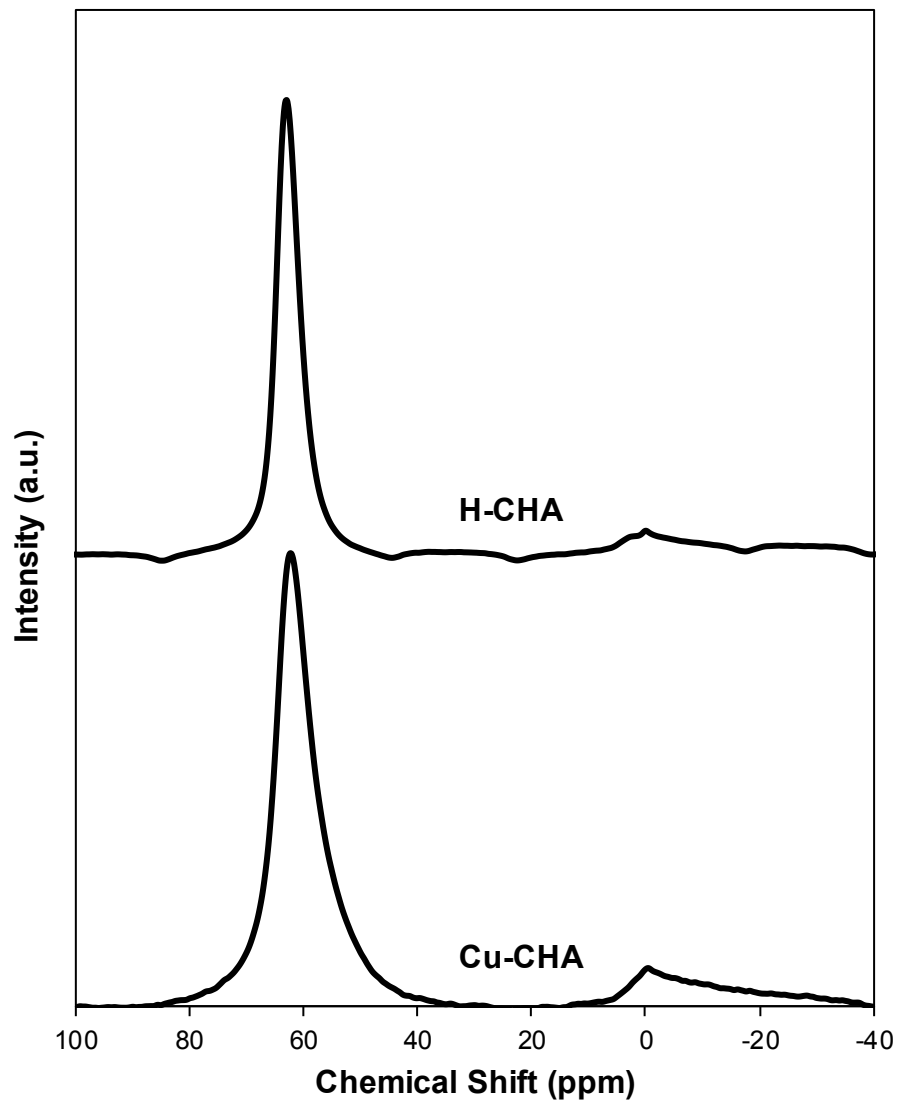


Figure S.3.2. ^{27}Al MAS NMR spectra of H-CHA and Cu-CHA.

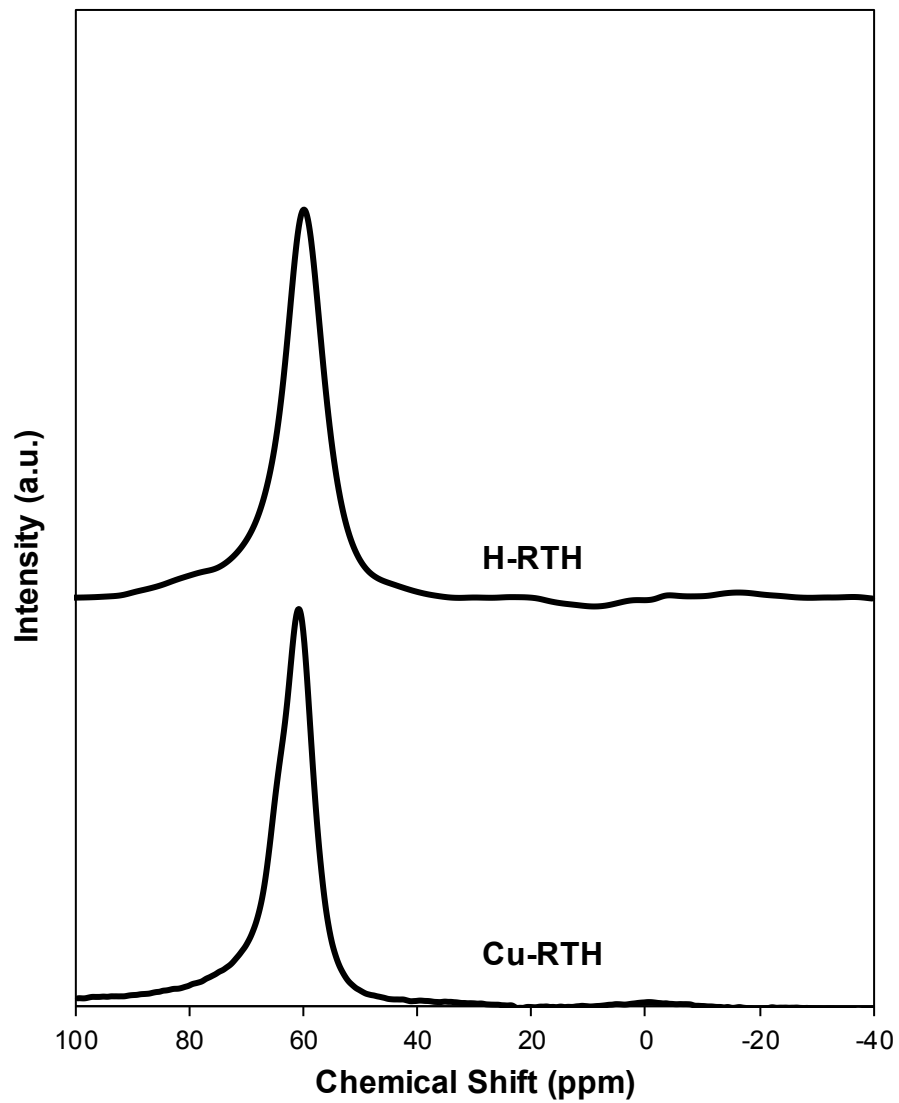


Figure S.3.3. ^{27}Al MAS NMR spectra of H-RTH and Cu-RTH.

Section S.4. IR Spectra of H-RTH Before and After NH₃ Exposure

In situ IR experiments were performed to monitor interactions of H⁺ sites in H-RTH (Si/Al = 15) with NH₃. H-RTH was pressed into a self-supporting wafer (~0.40 g) and placed within an *operando* FTIR cell, using a procedure that has been described elsewhere.⁷ The sample was heated to 723 K and held for 2 h under 50 mL min⁻¹ of 10% O₂ (99.5%, Indiana Oxygen) and balance N₂ (99.999% UHP, Indiana Oxygen), and then cooled to 433 K under flow (10% O₂ and balance N₂) to give the spectra (dark traces) in Figure S.4 (OH stretching region shown in Fig. S.4.1, NH bending region shown in Fig. S.4.2). The H-RTH wafer was then saturated in flowing NH₃ (350 ppm, 3 h, 433 K), to give the spectra (light traces) in Figure S.4. After NH₃ saturation, Brønsted OH bands disappeared completely, and new IR bands for NH₄⁺ bending vibrations at 1425 cm⁻¹ appeared concomitantly. These data indicate that all H⁺ sites in H-RTH were titrated by NH₃, and that the H⁺/Al_f value of 0.61 measured in NH₃ TPD experiments does not reflect a fraction of H⁺ sites that were inaccessible to NH₃.

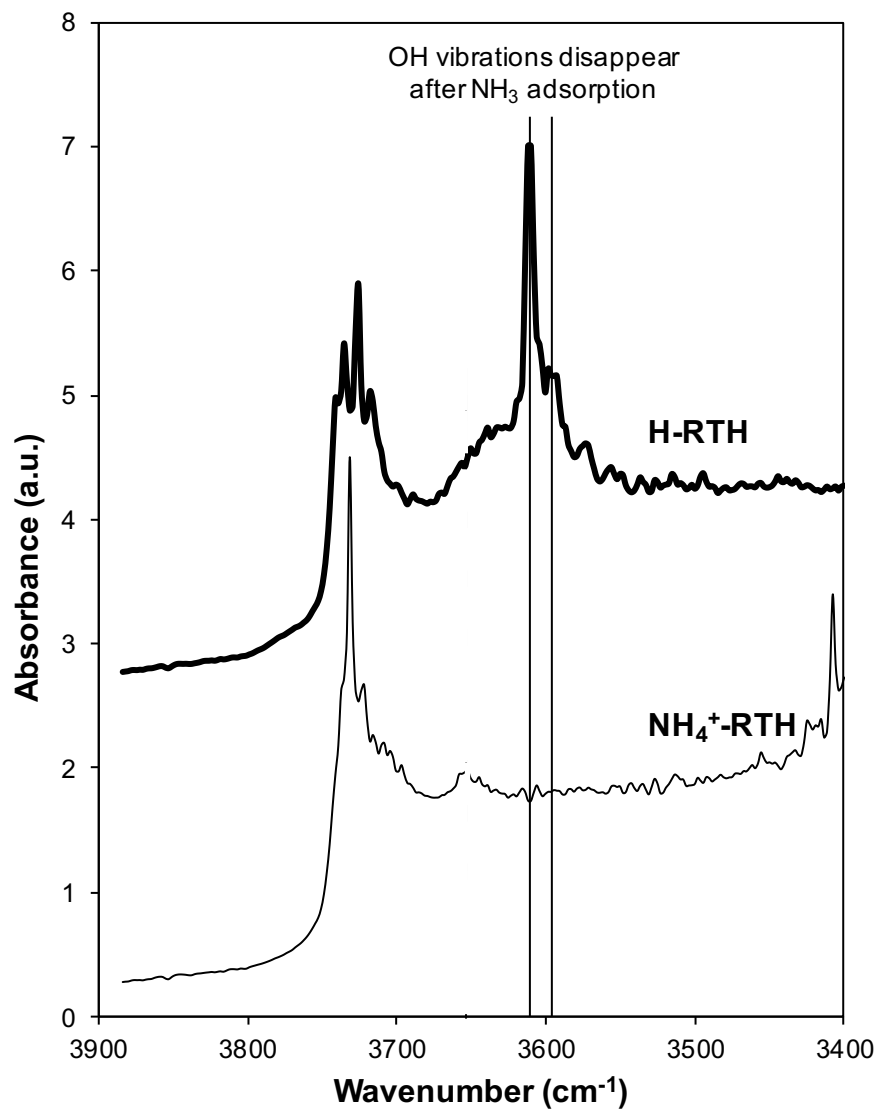


Figure S.4.1. IR spectra (OH stretching region: 3400-3900 cm⁻¹) of H-RTH at 433 K before (dark) and after (light) NH₃ saturation.

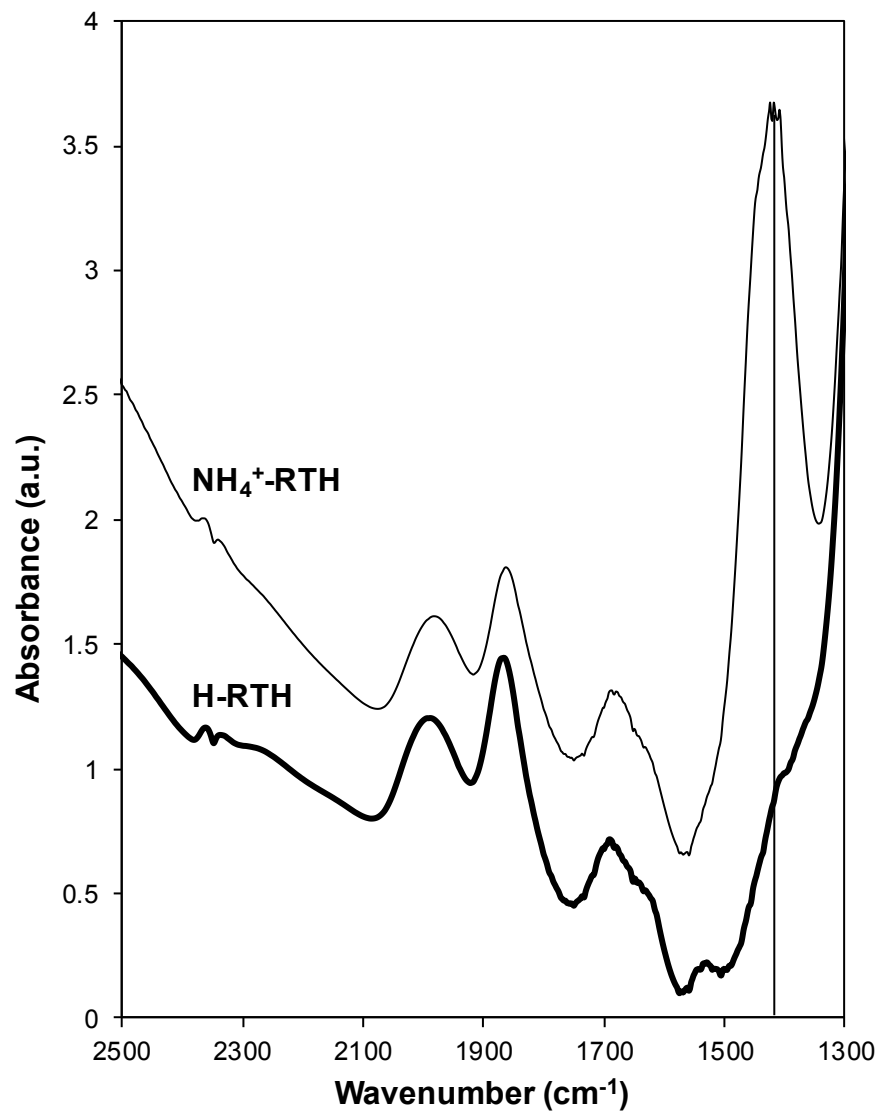


Figure S.4.2. IR spectra (N-H bending region: 1300-2500 cm⁻¹) of H-RTH at 433 K before (dark) and after (light) NH₃ saturation.

Section S.5. NH₃ TPD on Cu-zeolites

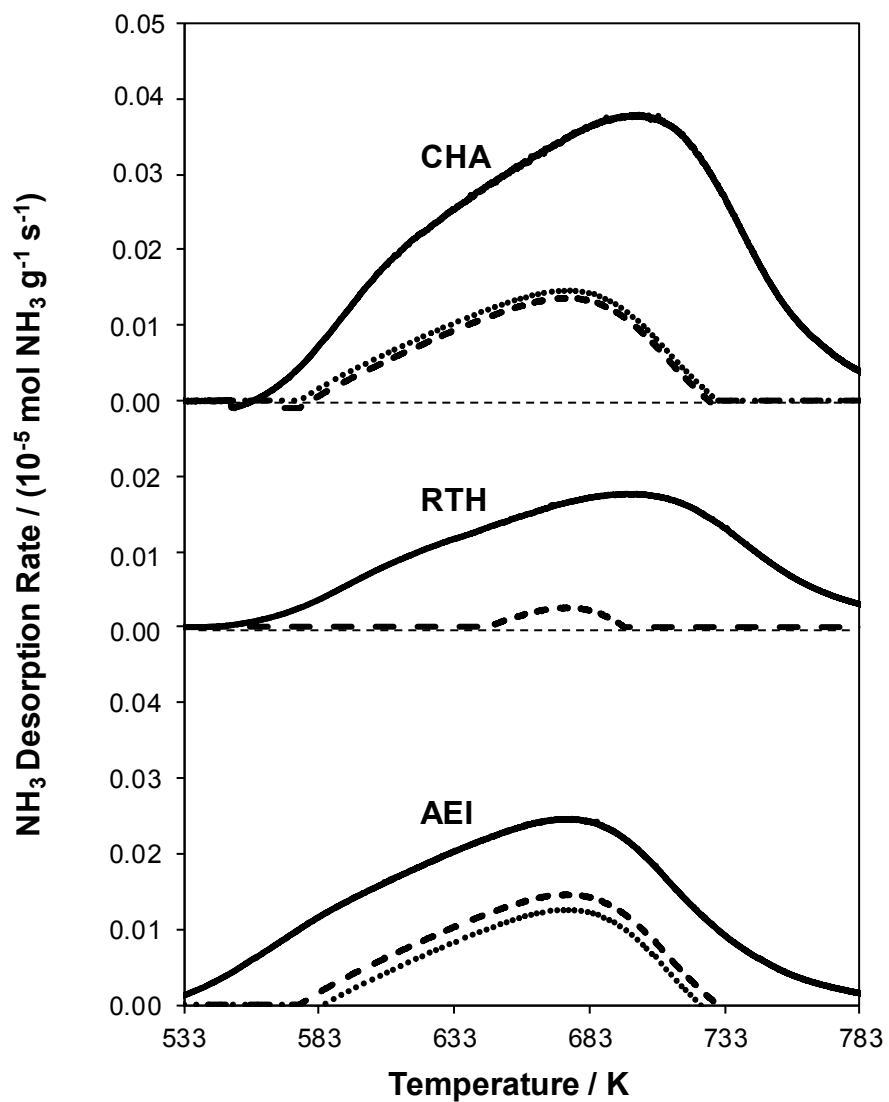


Figure S.5. NH₃ desorption rates as a function of temperature on fresh Cu-form after SCR (solid), aged Cu-form before SCR (dashed) and aged Cu-form after SCR (dotted) on CHA, RTH, and AEI zeolites.

Section S.6. References

- 1 J. Klinowski, *Prog. NMR Spectrosc.*, 1984, **16**, 237–309.
- 2 J. H. Kwak, J. Z. Hu, D. H. Kim, J. Szanyi and C. H. F. Peden, *J. Catal.*, 2007, **251**, 189–194.
- 3 A. Omega, J. A. van Bokhoven and R. Prins, *J. Phys. Chem. B*, 2003, **107**, 8854–8860.
- 4 A. Omega, R. Prins and J. A. Van Bokhoven, *J. Phys. Chem. B*, 2005, **109**, 9280–9283.
- 5 R. Gounder, A. J. Jones, R. T. Carr and E. Iglesia, *J. Catal.*, 2012, **286**, 214–223.
- 6 Z. Luv and A. J. Vega, *J. Phys. Chem.*, 1987, **91**, 374–382.
- 7 J. Wang, V. F. Kispersky, W. N. Delgass and F. H. Ribeiro, *J. Catal.*, 2012, **289**, 171–178.